Chapter

Magneto-Hydrodynamic Natural Convection Flow in a Concentric Annulus with Ramped Temperature and Ramped Motion of the Boundaries

Khadijah Lawal and Haruna Jibril

Abstract

An unsteady MHD flow of a temperature dependent heat source/sink in an annulus due to ramped motion and ramped temperature of the boundaries has been analyzed. The partial differential equations of the fluid flow are formulated taking into account the ramped temperature and ramped velocity of the inner cylinder. The closed form solution are obtained for three cases of the magnetic field being fixed relative the fluid, cylinder and when the velocity of the magnetic field is less than the velocity of the moving cylinder. The problem is solved using Laplace transform technique to obtain the Laplace domain solution and Riemann sum approximation to obtain the time domain solution. The effect of the governing parameters on the fluid flow are illustrated graphically. It is found that, Hartmann number has a retarding effect on the skin friction at the outer surface of the inner cylinder and mass flow rate. It also decreases fluid velocity for cases $(K = 0.0 \; and \; K = 0.5)$ the reverse effect is noticed for case $(K = 1.0)$. Increase in Hartmann number lead to an increase in skin friction at the inner surface of the outer cylinder for case $(K = 0.0)$ but decreases it for cases $(K = 0.0 \; and \; K = 0.5)$.

Keywords: ramped temperature, ramped motion, magneto-hydrodynamic, natural convection, annulus, heat source/sink

1. Introduction and definition of terms

Magneto-hydrodynamics (MHD) is the study of the motion of electrically conducting fluid. The study of magneto-hydrodynamic plays an important role in agriculture, engineering and petroleum industries. For instance, it may be used to deal with problems such as cooling of nuclear reactor by liquid sodium. The importance of MHD cannot be over emphasized. MHD has applications in many areas like the earth, sun, industry, fusion etc.

To appreciate the importance of fluid dynamics in life demands little more than just a glance around us. In general, life as we know would not exist if there are no

fluids and the behavior they exhibit. The water and air we respectively drink and breathe are fluids. In addition, our body fluids are mostly water based. As a matter of fact, our body system is made up of about 75% of fluid which helps in regulating the activities of the body system ranging from body temperature control to waste removal. In a more practical setting, like in our transportation systems, recreation, entertainment (sound from radio speakers) and our sleep (water beds), fluids greatly influence our comfort. It is clear to see from this that engineers need a clear knowledge of fluid behavior to handle many systems of their encounter.

Over the past decades, studies have been carried out on magneto-hydrodynamic natural convection in an annulus under different physical situations and geometry. This is because of its applications in nature, engineering, industries and technologies. These applications include but not limited to underground disposal of radioactive waste materials, storage of foodstuffs, exothermic and/or endothermic chemical reactions, heat removal from nuclear fuel debris, dissociating fluids in packed bed reactors, aerodynamics, geothermal energy extraction, purification of crude oil and spacecraft, MHD generators, MHD flow meters and MHD pump.

- **Magneto-hydrodynamics (MHD):** Magneto-hydrodynamics is the study of electrically conducting fluids in the presence of magnetic and electric fields, example, plasma, liquid metals and salt water.

- **Free or Natural Convection:** Free or Natural convection is the process when a temperature difference produces a density difference which results in mass movement.

- **Forced convection:** Is a mechanism or form of heat transport in which fluid motion is generated by an external source (like suction device fan and pump).

- **Mixed convection:** Is the type of heat transport caused by both natural and force convections.

- **Ramped temperature:** Is the gradual rate of change in temperature over time expressed in degree per second.

- **Ramped motion:** Is a gradual transition in any flow parameter that can be animated from the start value to the end. The length of the ramp behavior in the time line defines the speed of the transition by the behavior's end value.

- **Heat sink:** Is any environment or medium that absorb heat. It decreases the heat of the fluid on the cylinder by an external agent. It is an environment capable of absorbing heat from substance within it and with which it is in thermal contact, without an appreciable change in its own phase.

- **Heat source:** Is any device or natural body that supplies heat. Is the increase of heat of the fluid on the cylinder by an external agent from the place or the environment which heat is obtained.

- **Annulus**: Annulus is the area bounded by two concentric cylinders.

The presence of magnetic field on a Couette flow induces a Lorentz force which either accelerates or decelerates the flow element between the planes which depend on the electrical properties of the plane. The need to control the motion of the boundary layer is one motivation for this study. In many technological phenomena,

such as earth core, aeronautics etc. the motion of a system initially start with an accelerated velocity and then after some time moves with almost constant velocity. This prompted us to consider the ramped like motion of a concentric cylinder and analyze the flow formation.

Chandran *et al.* [1] studied natural convection near a vertical plate with ramped wall temperature and they obtained two different solutions, one valid for Prandtl number different from unity and the other for which the Prandtl number is unity. They concluded that the solutions for dimensional velocity and temperature variables depend upon the Prandtl number of the fluid and the expression of the fluid velocity is not uniformly valid for all values of Prandtl number. In their work, heat generating/absorption is absent. However, when the temperature differences are appreciably large, the volumetric heat generation/absorption term may exert strong influence on the heat transfer and as a consequence on the fluid flow as well. Jha *et al.* [2] studied natural convection flow of heat generating or absorbing fluid near a vertical plate with ramped temperature and consider two cases, plate with continuous ramped temperature and the other with isothermal temperature. They concluded that the isothermal case is always higher than the ramped case. The above mentioned works are carried out in the absence of magnetic field. Seth and Ansari [3] considered hydro-magnetic natural convections flow past an impulsively moving vertical plate embedded in a porous medium with ramped wall temperature in the presence of thermal diffusion with heat absorption. Nandkeolyar and Das [4] studied unsteady MHD free convection flow of a heat absorbing dusty fluid past a flat plate with ramped wall temperature. Seth and Nandkeolyar [5] studied MHD natural convection flow with radiative heat transfer past an impulsively moving plate with ramped wall temperature. Again, Seth et al. [6] investigated hydro-magnetic natural convection flow with heat and mass transfer of a chemically reacting and heat absorbing fluid past an accelerated moving plate with ramped temperature and ramped surface concentration through a porous medium. Recently, Khadijah and Jibril [7] studied Unsteady MHD natural convection flow of heat generating/absorbing fluid near a vertical plate with ramped temperature and motion. In the same year, Khadijah and Jibril [8] investigated Time dependent MHD natural convection flow of a Heat generating/absorbing fluid near a vertical porous plate with ramped boundary conditions.

Jha and Jibril [9] investigated hydro-magnetic flow due to ramped motion of the boundary. In their work they studied the effect of magnetic field on velocity and skin friction, due to ramped motion of the horizontal plate and it was concluded that the ramped motion are less compared to the constant motion. However, the effect of ramped temperature profile was not considered. Kumar and Singh [10] studied the transient magneto hydrodynamic Couette flow with ramped velocity. The velocity of the magnetic field, applied perpendicular to the plate is taken to be different from the velocity of the lower plate (the lower plate is moving with ramped velocity). It was concluded that the effect of the velocity on the magnetic field is to increase the velocity of the fluid from the upper plate to the lower plate Jha and Jibril [11] studied the effects of transpiration on the MHD flow near a porous plate having ramped motion. In their work they compare flow formation due to ramped motion of porous plate with the flow formation due to constant motion of the porous plate. Jha and Jibril [12] studied the time dependent MHD Couette flow due to ramped motion of one of the boundaries. It was found that velocity and skin friction increases with an increase of Hartman number when the magnetic field is fixed with respect to the moving plate. While the reverse when it is fixed with respect to the fluid. Jha and Jibril [13] investigated the unsteady hydro-magnetic Couette flow due to ramped motion of the porous plate. The aforementioned works were carried out on a horizontal plate.

Jha and Apere [14] on the other hand investigated Unsteady MHD Couette flow in an annulus, by applying Riemann-sum approximation approach to obtain the Laplace inversion of their solution in time domain. Jha and Apere [15] studied unsteady MHD two-phase Couette flow of fluid particles suspension in an annulus. In their work, they employed the D'Alermbert method used by Reccebli and kurt in conjunction of Riemann sum approximation method for both cases of the magnetic field being fixed to either the fluid or the moving cylinder to obtain the solution of the problem. Anand [16] investigated the Effect of radial magnetic field on free convective flow over ramped velocity moving vertical inner cylinder with ramped type temperature and concentration. In the same year, Anand [17] studied the effect of radial magnetic field on natural convection flow in alternate conducting vertical concentric annuli with ramped temperature. Anand [18] studied the effect of velocity of applied magnetic field on natural convection over ramped type moving inner cylinder with ramped type temperature solved numerically by using implicit finite difference Crank–Nicolson method. They found out that, when velocity is employed to magnetic field, then effect of magnetic field gets reversed and the effect of velocity of magnetic field get more pronounced with radii ratio. Also, Hartmann number and time parameter have increasing effects on the skin-friction profile. Taiwo [19] investigated the exact solution of MHD natural convection flow in a concentric annulus with heat absorption. It is found that the magnitude of maximum fluid velocity is greater in the case of isothermal heating compared with the constant heat flux case when the gap between the cylinders is less or equal to radius of the inner cylinder. More also, the various values of the non-dimensional heat absorption parameter (A) and the corresponding values of annular gap are almost the same conditions. Other important researchers [20–28] investigated MHD flow under different physical geometry and thermal conditions of the boundaries.

To the best of the authors' knowledge, no studies have been reported concerning the combined effect of constant temperature, heat generating/absorbing parameter, MHD and ramped like motion of the inner cylinder and temperature in a concentric cylinder. The condition involving ramped like cylindrical motion appears in aerodynamics and oil refinement industry. Therefore, it is important to analyze the flow processes and try to understand the function of related mechanics of ramped moving vertical cylinder and ramped temperature.

2. Mathematical formulation

This research considers the time dependent natural convection flow of viscous, incompressible and electrically conducting fluid formed by two cylinders of infinite length with radius a and b such that $a < b$ under the influence of transverse magnetic field. The motion as well as the temperature of the inner cylinder is ramped while the motion together with the temperature of the outer cylinder is fixed. The z - axis is taken along the axis of the cylinder in the vertical upward direction and r'-axis is in the radial direction. A magnetic field of strength B_0 is assumed to be uniformly applied in the direction perpendicular to the direction of flow. In the present physical situation, a constant isothermal heating of $T_w$is applied at the outer surface of the inner cylinder such that $T_w > T_0$. When the time is greater than zero that is $t' > 0$, the temperature of the cylinder is increased or decreased to $T'_0 + \left(T'_w - T_0\right)\frac{t'}{t_0}$, and it begins to move with a velocity proportional to $f(t')$ when $t' \leq t_0$ and thereafter $t' > t_0$ is maintained at constant temperature T_w as presented in **Figure 1**.

The momentum and energy equations governing the present physical situation are given by;

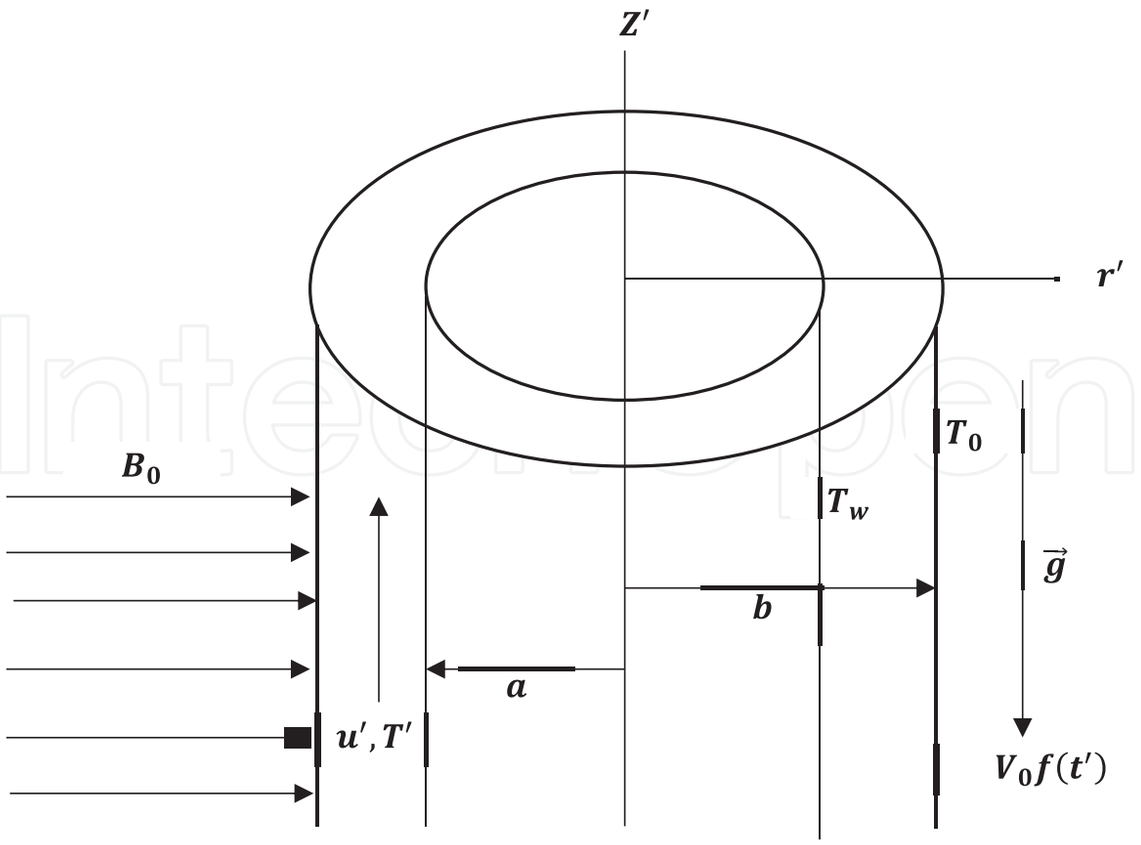

Figure 1.
Physical configuration.

$$\frac{\partial u'}{\partial t'} = \nu\left[\frac{\partial^2 u'}{\partial r'^2} + \frac{1}{r'}\frac{\partial u'}{\partial r'}\right] - \frac{\sigma {B_0}^2 u'}{\rho} + g\beta(T' - T_0) \tag{1}$$

This is valid when the magnetic lines of force are fixed relative to the fluid. If the magnetic field is also having ramped motion with the same velocity as the moving cylinder, the relative motion must be accounted for. In this case the Eq. (1) above is replaced by:

$$\frac{\partial u'}{\partial t'} = \nu\left[\frac{\partial^2 u'}{\partial r'^2} + \frac{1}{r'}\frac{\partial u'}{\partial r'}\right] - \frac{\sigma {B_0}^2}{\rho}(u' - V_0 f(t')) + g\beta(T' - T_0) \tag{2}$$

This is valid when the magnetic lines of force are fixed relative to the moving cylinder. Eqs. (1) and (2) can be combined to obtain the momentum and energy equation respectively.

$$\frac{\partial u'}{\partial t'} = \nu\left[\frac{\partial^2 u'}{\partial r'^2} + \frac{1}{r'}\frac{\partial u'}{\partial r'}\right] - \frac{\sigma {B_0}^2}{\rho}(u' - Kf(t')) + g\beta(T' - T_0) \tag{3}$$

$$\frac{\partial T'}{\partial t'} = \frac{k}{\rho c_p}\left[\frac{\partial^2 T'}{\partial r'^2} + \frac{1}{r'}\frac{\partial T'}{\partial r'}\right] + \frac{Q}{\rho c_p} \tag{4}$$

The relevant dimensional boundary conditions are;

$$t' \le 0 \qquad u' = 0, \quad T' = T_0 \quad \text{For } a \le r' \le b$$

$$t' > 0 \qquad \begin{cases} u' = U_0 f(t'), \quad T' = T'_0 + \left(T'_w - T_0\right) f(t') & \text{at } r' = a \\ u' = 0, \quad T' = T_w & \text{at } r' = b \end{cases}$$

Where,

$$K = \begin{cases} 0 \text{ if the magnetic field is fixed relative to the fluid} \\ 0.5 \text{ if the velocity of the magnetic field is less than the velocity of the moving cylinder} \\ 1 \text{ if the magnetic field is fixed relative to the moving cylinder} \end{cases}$$

Anand and Kumar [10].

2.1 Non-dimensionalization

The following non-dimensional parameters are defined as:

$$t = \frac{t'\nu}{a^2}, \quad t_0 = \frac{a^2}{v}, \quad R = \frac{r'}{a}, \quad \lambda = \frac{b}{a}, \quad M^2 = \frac{\sigma {B_0}^2 a^2}{\rho\nu}, \quad \theta = \frac{(T' - T_0)}{(T_w - T_0)}, \quad Pr = \frac{\mu c_p}{k}$$

$$U = \frac{u'}{v_0}, \quad K = \frac{V_0}{U_0}, \quad U_0 = \frac{g\beta(T_w - T_0)a^2}{v}, \quad Gr = \frac{g\beta(T_w - T_0)a^3}{v^2}, \quad A = \frac{Q_0 V t_0}{k} \tag{5}$$

Where θ is the dimensionless temperature; Pr is the Prandtl number; M is the Hartmann number and t is the dimensionless time.

Using the non-dimensional parameters in Eq. (5) above, the governing equations of momentum (3) and energy (4) can be written in dimensionless form as:

$$\frac{\partial U}{\partial t} = \left[\frac{\partial^2 U}{\partial R^2} + \frac{1}{R}\frac{\partial U}{\partial R}\right] - M^2(U - K(f(t)) + Gr\theta \tag{6}$$

$$\frac{\partial \theta}{\partial t} = \frac{1}{Pr}\left[\frac{\partial^2 \theta}{\partial R^2} + \frac{1}{R}\frac{\partial \theta}{\partial R}\right] - A \tag{7}$$

The initial conditions for velocity and temperature field in dimensionless form are:

$$t \le 0 \qquad U = 0, \quad \theta = 0 \ \text{ For } \ 1 \le R \le \lambda \tag{8}$$

While the boundary conditions in dimensionless form is given as:

$$t > 0 \qquad \begin{cases} U = f(t), \quad \theta = f(t) & \text{at } R = 1 \\ U = 0, \quad \theta = 0 & \text{at } R = \lambda \end{cases} \tag{9}$$

Where $\lambda = \frac{b}{a} > 1$

$$f(t) = \begin{cases} \dfrac{t}{t_0} \ \textit{if } 0 \le t \le t_0 \\ 1 \ \ \textit{if } t \ge t_0 \end{cases}$$

$$f(t) = H(t)\left(\frac{t}{t_0}\right) - \left(\frac{1}{t_0}\right)(t - t_0)H(t - t_0)$$

Where $H(t)$ is the Heaviside unit step function defined by $H(t) = \begin{cases} 0, t < 0 \\ 1, t \ge 0 \end{cases}$

2.2 Laplace transform

Introducing the Laplace transform on the dimensionless velocity and temperature

$$\overline{U}(R,s) = \int_0^\infty U(R,t)\exp(-st)dt \tag{10}$$

$$\overline{\theta}(R,s) = \int_0^\infty \theta(R,t)\exp(-st)dt \tag{11}$$

(Where s is the Laplace parameter such that $s > 0$) applying the properties of Laplace transform on Eqs. (6) and (7) subject to initial condition (8) gives

$$\left[\frac{d^2\overline{U}}{dR^2} + \frac{1}{R}\frac{d\overline{U}}{dR}\right] - \left(M^2 + s\right)\overline{U} = -Gr\overline{\theta} - M^2K\overline{f}(s) \tag{12}$$

$$\left[\frac{d^2\overline{\theta}}{dR^2} + \frac{1}{R}\frac{d\overline{\theta}}{dR}\right] - sPr\overline{\theta} - \frac{HPr}{s} = 0 \tag{13}$$

The boundary conditions (8) becomes

$$\begin{aligned} &\overline{U} = \overline{f}(s), \quad \overline{\theta} = \overline{f}(s) \quad \text{at } R = 1 \\ &\overline{U} = 0, \quad \overline{\theta} = 0 \quad \text{at } R = \lambda \end{aligned} \tag{14}$$

2.3 Solution

The set of Bessel ordinary differential Eqs. (12) and (13) with the boundary condition (14) are solved for velocity and temperature in the Laplace domain as follows:

$$\begin{aligned} \overline{U}(R,s) &= C_3 I_0\left(R\sqrt{M^2+s}\right) + C_4 K_0\left(R\sqrt{M^2+s}\right) \\ &- \left[\frac{Gr\left(C_1 I_0\left(R\sqrt{sPr}\right) + C_2 K_0\left(R\sqrt{sPr}\right)\right)}{sPr - \left(M^2+s\right)}\right] + \frac{M^2K\overline{f}(s)}{M^2+s} - \frac{GrH}{\left(M^2+s\right)s^2} \end{aligned} \tag{15}$$

$$\overline{\theta}(R,s) = C_1 I_0\left(R\sqrt{sPr}\right) + C_2 K_0\left(R\sqrt{sPr}\right) - \frac{A}{s^2} \tag{16}$$

Where;

$$C_1 = \frac{s^2\overline{f}(s)K_0\left(\lambda\sqrt{sPr}\right) + A\left[K_0\left(\lambda\sqrt{sPr}\right) - K_0\left(\sqrt{sPr}\right)\right]}{s^2\left[I_0\left(\sqrt{sPr}\right)K_0\left(\lambda\sqrt{sPr}\right) - I_0\left(\lambda\sqrt{sPr}\right)K_0\left(\sqrt{sPr}\right)\right]}$$

$$C_2 = \frac{s^2\overline{f}(s)I_0\left(\lambda\sqrt{sPr}\right) + A\left[I_0\left(\lambda\sqrt{sPr}\right) - I_0\left(\sqrt{sPr}\right)\right]}{s^2\left[K_0\left(\sqrt{sPr}\right)I_0\left(\lambda\sqrt{sPr}\right) - K_0\left(\lambda\sqrt{sPr}\right)I_0\left(\sqrt{sPr}\right)\right]}$$

$$C_3 = \frac{\overline{f}(s)K_0(\lambda\delta) - A_1[K_0(\lambda\delta) - K_0(\delta)] + A_4[K_0(\lambda\delta) - K_0(\delta)] + [A_2K_0(\lambda\delta) - A_3K_0(\delta)]}{[I_0(\delta)K_0(\lambda\delta) - I_0(\lambda\delta)K_0(\delta)]}$$

$$C_4 = \frac{\overline{f}(s)I_0(\lambda\delta) - A_1[I_0(\lambda\delta) - I_0(\delta)] + A_4[I_0(\lambda\delta) - I_0(\delta)] + [A_2I_0(\lambda\delta) - A_3I_0(\delta)]}{[K_0(\delta)I_0(\lambda\delta) - K_0(\lambda\delta)I_0(\delta)]}$$

Where: $= \sqrt{M^2+s}$, $A_1 = \frac{M^2 K\bar{f}(s)}{M^2+s}$, $A_4 = \frac{GrA}{(M^2+s)s^2}$, $A_2 = \frac{Gr\left[C_1 I_0\left(\sqrt{sPr}\right)+C_2 K_0\left(\sqrt{sPr}\right)\right]}{sPr-\left(M^2+s\right)}$

$$A_3 = \frac{Gr\left[C_1 I_0\left(\lambda\sqrt{sPr}\right) + C_2 K_0\left(\lambda\sqrt{sPr}\right)\right]}{sPr - \left(M^2+s\right)}$$

2.4 Skin friction

The skin – friction is the measure of the frictional force between the fluid and the surface of the cylinder. $(\bar{\tau}_1)$ is the skin-friction at the outer surface of the inner cylinder and $(\bar{\tau}_\lambda)$ is the skin- friction at the inner surface of the outer cylinder. These are obtained by taking the first derivative of the velocity $\overline{U}(R,s)$ given in Eq. (15) with respect to R as follows:

$$\begin{aligned}\overline{\tau_1} = \left.\frac{d\overline{U}}{dR}\right|_{R=1} &= \sqrt{M^2+s}\left(C_3 I_1\left(\sqrt{M^2+s}\right) - C_4 K_1\left(\sqrt{M^2+s}\right)\right) \\ &- \frac{Gr\sqrt{sPr}}{\left[sPr-\left(M^2+s\right)\right]}\left(C_1 I_1\left(\sqrt{sPr}\right) - C_2 K_1\left(\sqrt{sPr}\right)\right)\end{aligned} \tag{17}$$

$$\begin{aligned}\overline{\tau_\lambda} = \left.\frac{d\overline{U}}{dR}\right|_{R=\lambda} &= \sqrt{M^2+s}\left(C_3 I_1\left(\lambda\sqrt{M^2+s}\right) - C_4 K_1\left(\lambda\sqrt{M^2+s}\right)\right) \\ &- \frac{Gr\sqrt{sPr}}{\left[sPr-\left(M^2+s\right)\right]}\left(C_1 I_1\left(\lambda\sqrt{sPr}\right) - C_2 K_1\left(\lambda\sqrt{sPr}\right)\right)\end{aligned} \tag{18}$$

2.5 Nusselt number

The expression for Nusselt number which is the measure of heat transfer rate on the cylinder is presented in the following form. $Nu_\alpha = \left.\frac{d\bar{\theta}}{dR}\right|_{R=\alpha}$

$$Nu_1 = \left.\frac{d\bar{\theta}}{dR}\right|_{R=1} = \sqrt{sPr}\left(C_1 I_1\left(\sqrt{sPr}\right) - C_2 K_1\left(\sqrt{sPr}\right)\right) \tag{19}$$

$$Nu_\lambda = \left.\frac{d\bar{\theta}}{dR}\right|_{R=\lambda} = \sqrt{sPr}\left(C_1 I_1\left(\lambda\sqrt{sPr}\right) - C_2 K_1\left(\lambda\sqrt{sPr}\right)\right) \tag{20}$$

2.6 Mass flow rate

Mass flow rate evaluates the rate of fluid flow through the annulus. It is achieved by taking a definite integral of Eq. (15) with respect to R as shown below:

$$\begin{aligned}\overline{Q} = 2\pi\int_1^\lambda R\overline{U}(R,s)dR &= 2\pi\frac{C_3}{\sqrt{M^2+s}}\left(\lambda I_1\left(\lambda\sqrt{M^2+s}\right) - I_1\left(\sqrt{M^2+s}\right)\right) \\ &- \frac{C_4}{\sqrt{M^2+s}}\left(\lambda K_1\left(\lambda\sqrt{M^2+s}\right) - K_1\left(\sqrt{M^2+s}\right)\right) - \frac{GrC_1}{\sqrt{sPr\left[SPr-\left(M^2+s\right)\right]}}\left(\lambda I_1\left(\lambda\sqrt{sPr}\right) - I_1\left(\sqrt{sPr}\right)\right) \\ &+ \frac{GrC_2}{\sqrt{sPr\left[sPr-\left(M^2+s\right)\right]}}\left(\lambda K_1\left(\lambda\sqrt{sPr}\right) - K_1\left(\sqrt{sPr}\right)\right) \\ &+ \left(\frac{\lambda^2-1}{2}\right)\left(\frac{M^2 K\bar{f}(s)}{M^2+s}\right) - \left(\frac{\lambda^2-1}{2}\right)\left(\frac{GrA}{(M^2+s)s^2}\right)\end{aligned} \tag{21}$$

2.7 Riemann sum approximation

Eqs. (15) and (16) are to be inverted in order to determine the velocity and temperature in time domain. Since these equations are difficult to invert in closed form. We use a numerical procedure used in Jha and Apere [14] which is based on the Riemann-sum approximation. In this method, any function in the Laplace domain can be inverted to the time domain as follows.

$$U(R,t) = \frac{e^{\varepsilon t}}{t}\left[\frac{1}{2}\overline{U}(R,\varepsilon) + Re\sum_{n=1}^{M}\overline{U}\left(R,\varepsilon + \frac{in\pi}{t}\right)(-1)^n\right], 1 \le R \le \lambda \tag{22}$$

where Re refers to the real part of $i = \sqrt{-1}$ the imaginary number. M is the number of terms used in the Riemann-sum approximation and ε is the real part of the Bromwich contour that is used in inverting Laplace transforms. The Riemann-sum approximation for the Laplace inversion involves a single summation for the numerical process, its accuracy depends on the value of ε and the truncation error dictated by M. According to Tzou [29], the value of εt that best satisfied the result is 4.7.

2.8 Validation of results

In order to validate the results obtained from the Riemann sum approximation methods we use the partial differential equation parabolic and elliptic (PDEPE) method and compared the result. In General, it is given in the form:

$$c\left(x,t,u,\frac{\partial u}{\partial t}\right)\frac{\partial u}{\partial t} = x^{-m}\frac{\partial}{\partial x}\left(x^m f\left(x,t,u,\frac{\partial u}{\partial x}\right)\right) + s\left(x,t,u,\frac{\partial u}{\partial x}\right) \tag{23}$$

Initial condition $U(x,t_0) = U_0 x$ Boundary conditions- one at each boundary $(x,t,u) + q(x,t)f\left(x,t,u,\frac{\partial u}{\partial x}\right) = 0$. These comparisons are analyzed on the tables.

2.9 Result and discussion

A MATLAB program is written in order to depict the effect of the flow parameters such as the Hartman number (M), Prandlt number (Pr), Grashoff number (Gr), Heat source/sink parameter (A) and ratio of radii (λ) on Velocity (U), Temperature (T), Nusselt number at the outer surface of the inner cylinder (Nu_1), Nusselt number at the inner surface of the outer cylinder (Nu_λ), Skin friction (λ) at the outer surface of the inner cylinder (τ_1), Skin friction at the inner surface of the outer cylinder (τ_λ) and mass flow rate (Q).

Figure 2 illustrated the temperature profile for different values of time. It is seen from this graph that the temperature increases with increase in time. Increase in radii ratio lead to an increase in temperature as show in **Figure 3**. As the heat generating or absorbing parameter increase, a decrease in temperature is noticed as depicted in **Figure 4**.

Figure 5 illustrated the effect of time on fluid velocity for cases ($K = 0.0$ if the magnetic field is fixed relative to the fluid), ($K = 0.5$ if the velocity of the magnetic field is less than the velocity of the moving cylinder) and ($K = 1.0$ if the magnetic field is fixed relative to the moving cylinder) and for Prandtl number ($Pr = 0.71$ *Air and* $Pr = 7.0$ *Water*). These graphs show that the fluid velocity

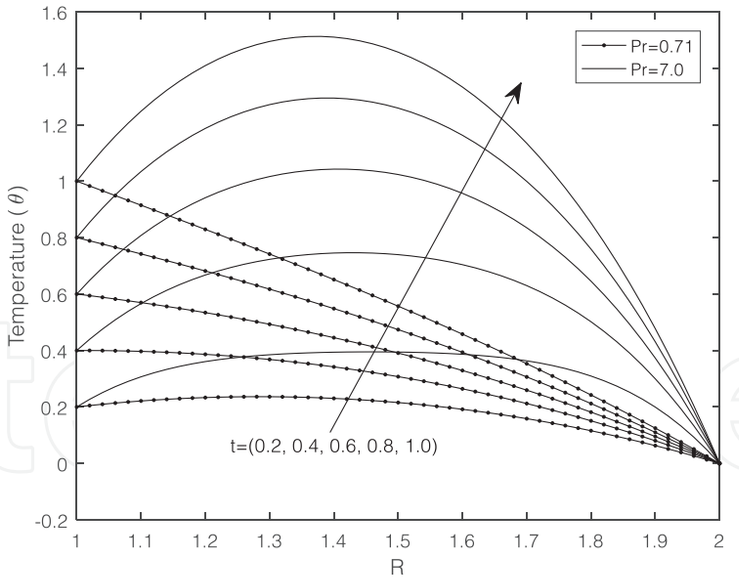

Figure 2.
Temperature distribution for different values of time $(t)(\lambda = 2.0, A = -2.0)$.

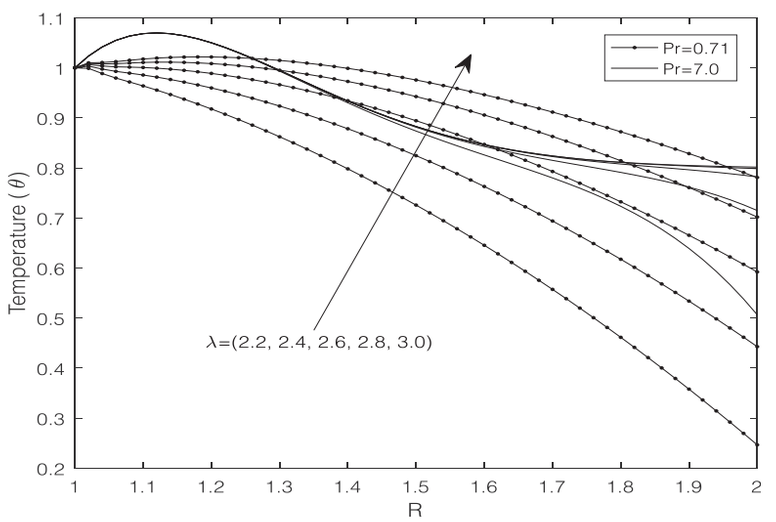

Figure 3.
Temperature distribution for different values of radii ratio (λ) $(t = 0.4, A = -2.0)$.

increase as time increases for all cases. It is interesting to note that, $Pr = 0.71$ converges faster than $Pr = 7.0$. Also, the value of velocity becomes higher as the value of K increases. **Figure 6** depicted the influence of Hartmann number on the fluid velocity for cases $(K = 0.0, K = 0.5\ and\ K = 1.0)\ and\ Pr = 7.0$. the fluid velocity decreases for cases $K = 0.0\ and\ K = 0.5$ This is physically true because application of magnetic field to an electrically conducting fluid give rise to resistivity force which is known as Lorentz force, this force has the tendency to decelerate fluid flow in the boundary layer region. Hartman number increase the fluid velocity for case $K = 1.0$. This implies that the magnetic field is supporting the fluid motion. Although a flow reversal is noticed for $= 7.0\ atR > 1.4$. **Figure 7** show the outcome of radii ratio on fluid velocity for cases $(K = 0.0, K = 0.5\ and\ K = 1.0)$ respectively and for $Pr = 7.0$. It is evident from the graph that, increase in radii ratio result to an increase in fluid velocity for all cases of K considered. The value of velocity becomes higher as the value of K increases. Heat generating/absorbing parameter (A) has a decreasing influence on the fluid velocity for all cases considered

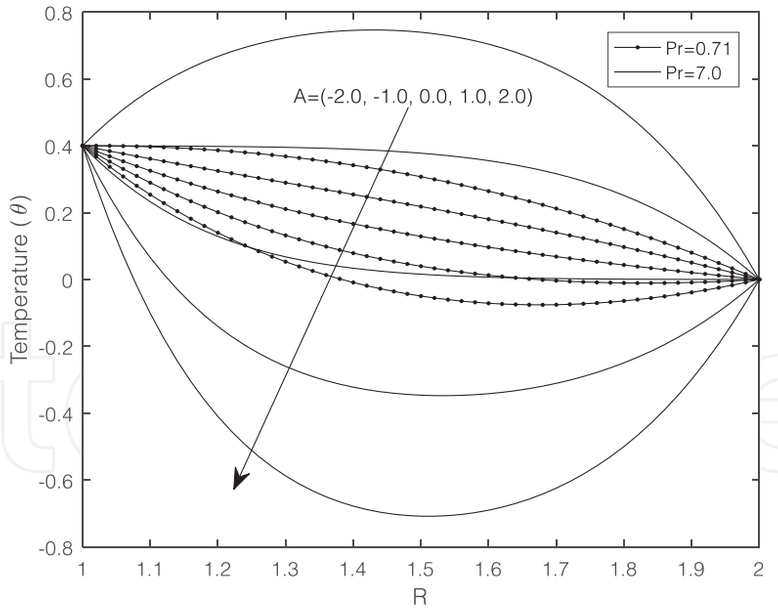

Figure 4.
Temperature profile for different values of heat source/sink (A) ($t = 0.4, \lambda = 2.0$).

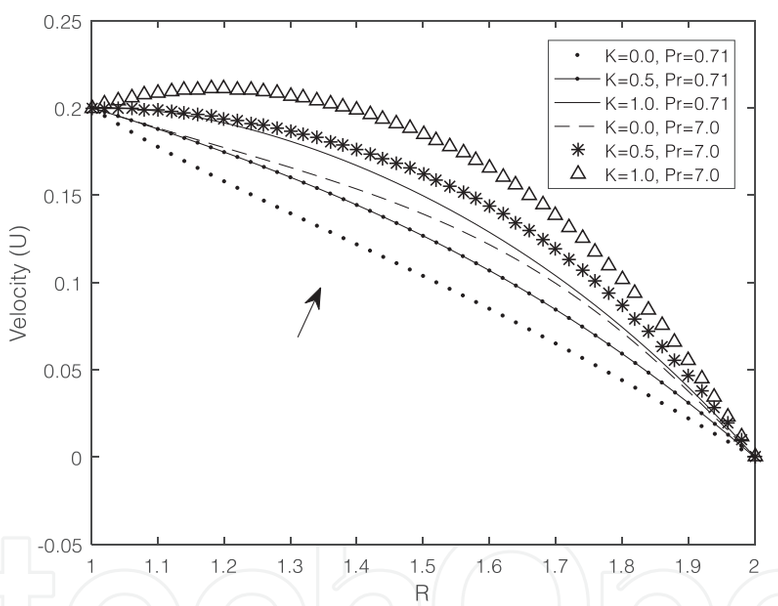

Figure 5.
Velocity distribution for different values of time (t and K)($Pr = 7.0, \lambda = 2.0, M = 2.0\ Gr = 5.0, A = -2.0$).

($K = 0.0, K = 0.5$ *and* $K = 1.0$) as illustrated in **Figure 8**. **Figure 9** presents the effect of Grashof number on fluid velocity for cases ($K = 0.0, K = 0.5$ *and* $K = 1.0$) and for $Pr = 7.0$. It is evident from the graph that increase in thermal buoyancy force lead to an increase in the fluid velocity for all cases of K.

Figure 10 presents the effect of Hartmann number on skin friction at the outer surface of the inner cylinder(τ_1) for cases ($K = 0.0, K = 0.5$ *and* $K = 1.0$) and for($Pr = 7.0$). It is evident from the graph that, the Hartmann number decrease the skin friction (τ_1) for all cases of K. **Figure 11** describe the impact of radii ratio on the skin friction (τ_1) for cases ($K = 0.0, K = 0.5$ *and* $K = 1.0$) and for($Pr = 7.0$). The graph show that, increase in radii ratio result to an increase in skin friction (τ_1). **Figure 12** depicts the influence of heat generating/absorbing parameter (A) for for cases ($K = 0.0, K = 0.5$ *and* $K = 1.0$) and for ($Pr = 7.0$). It is noticed from these

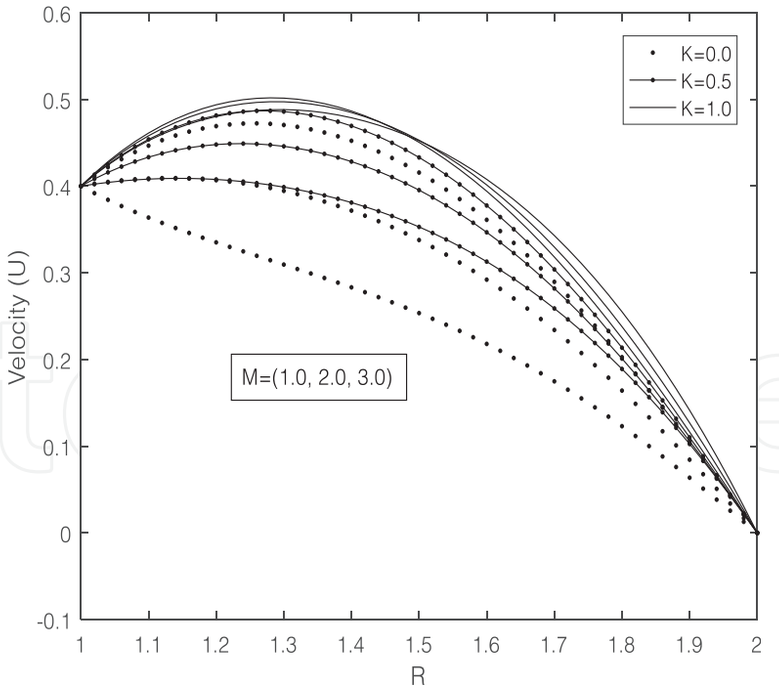

Figure 6.
Velocity distribution for different values of Hartmann number $(M \text{ and } K)$ $(Pr = 7.0, \lambda = 2.0, t = 0.4$ $Gr = 5.0, A = -2.0)$.

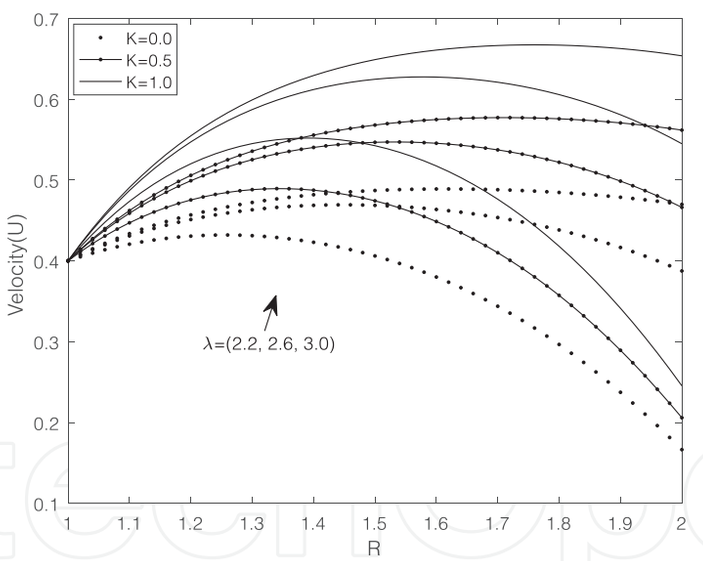

Figure 7.
Velocity distribution for different values of radii ratio $(\lambda \text{ and } K)$ $(Pr = 7.0, A = -2.0, t = 0.4\ Gr = 5.0, M = 2.0)$.

graphs that, Heat absorption has a retarding effect on the skin friction (τ_1) for all cases of K. It is essential to note that, a reverse flow occur on $Pr = 7.0$ at $t = 0.8$ for all cases of K considered. **Figure 13** illustrate the effect of Grashof number on skin friction (τ_1) for cases $(K = 0.0, K = 0.5 \textit{ and } K = 1.0)$ and for $(Pr = 7.0)$. The thermal buoyance force is seen to increase the skin friction (τ_1) from the graph. **Figure 14** depict the effect of Hartmann number on skin friction at the inner surface of the outer cylinder (τ_λ) for cases $(K = 0.0, K = 0.5 \textit{ and } K = 1.0)$ and for $(Pr = 7.0)$. It is seen from the graph that, Hartmann number increase the skin friction(τ_λ) for case $K = 0.0$ while the opposite effect is noticed for both case

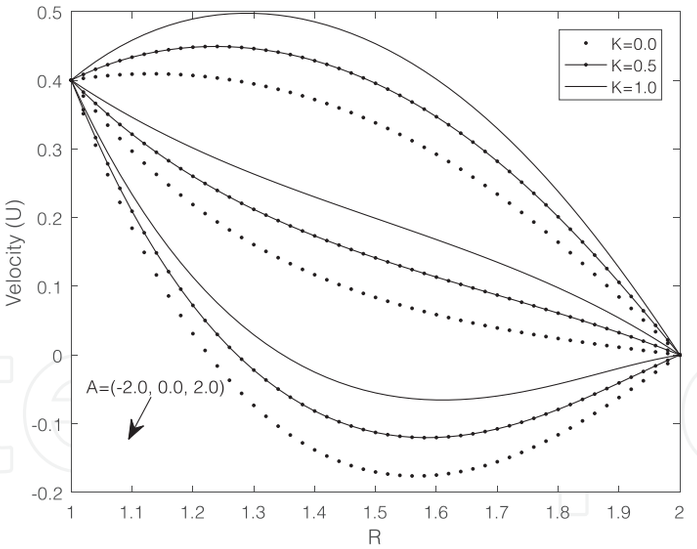

Figure 8.
Velocity distribution for different values of heat source/sink $(A \text{ and } K)$ $(Pr = 7.0, \lambda = 2.0, t = 0.4$ $Gr = 5.0, M = 2.0)$.

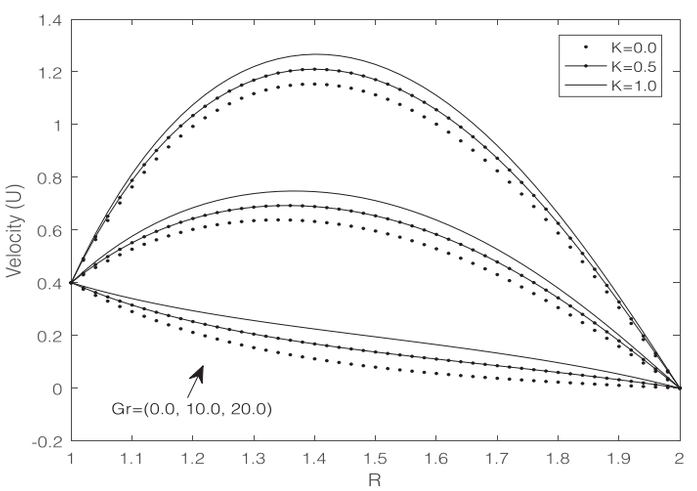

Figure 9.
Velocity distribution for different values of Grashof number $(Gr \text{ and } K)$ $(Pr = 7.0, \lambda = 2.0, t = 0.4,$ $A = -2.0, M = 2.0)$.

$K = 0.5$ *and* $K = 1.0$. **Figure 15** show the impact of radii ratio on the skin friction (τ_λ) for cases $(K = 0.0, K = 0.5$ *and* $K = 1.0)$ and for $(Pr = 7.0)$. The graph show that, increase in radii ratio lead to a decrease in skin friction (τ_λ). **Figure 16** present the influence of heat generating/absorbing parameter (A) for cases $(K = 0.0, K = 0.5$ *and* $K = 1.0)$ and for $(Pr = 7.0)$. It is evident from the graph that, there is an enhancement in skin friction(τ_λ) as the heat generating/absorbing parameter increase for all cases of K. **Figure 17** demonstrate the effect of Grashof number on skin friction (τ_λ) for cases $(K = 0.0, K = 0.5$ *and* $K = 1.0)$ and for $(Pr = 7.0)$. The thermal buoyance force is seen to decrease the skin friction (τ_λ) from the graph.

Figure 18 illustrate the effect of Hartmann number on mass flow rate (Q) for cases $(K = 0.0, K = 0.5$ *and* $K = 1.0)$ and for $(Pr = 7.0)$. The Hartman number decreases the volume flow rate. **Figure 19** show the impact of radii ratio on mass flow rate (Q) for cases $(K = 0.0, K = 0.5$ *and* $K = 1.0)$ and for $(Pr = 7.0)$. It is seen

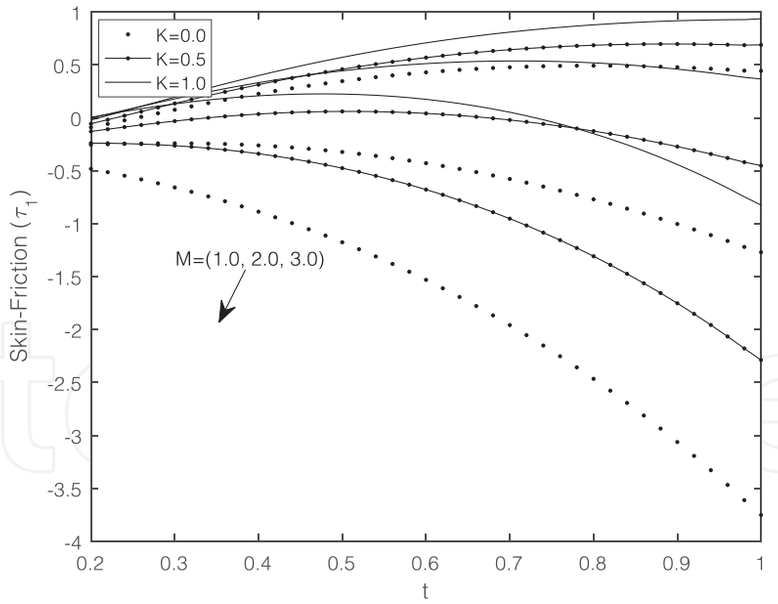

Figure 10.
Variation of skin friction (τ_1) *for different values of Hartmann number* $(M$ *and* $K)(Pr = 7.0, A = -2.0,$ $\lambda = 2.0$ $Gr = 5.0)$.

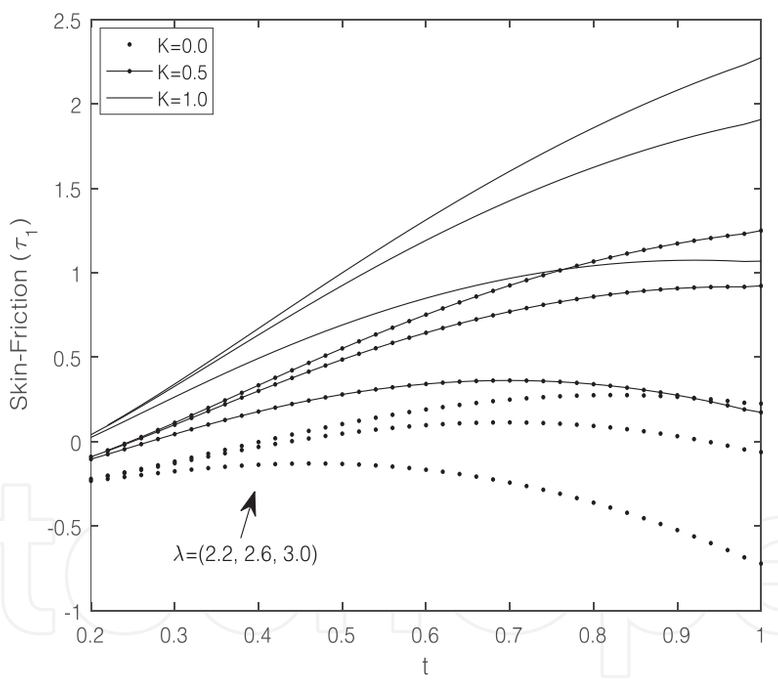

Figure 11.
Variation of skin friction (τ_1) *for different values of radii ratio* $(\lambda$ *and* $K)$ $(Pr = 7.0, A = -2.0, M = 2.0$ $Gr = 5.0)$.

from the graph that, the radii ratio increase the mass flow rate for all cases of K. **Figure 20** present the influence of heat generating/absorbing parameter on mass flow rate (Q) for cases $(K = 0.0, K = 0.5$ *and* $K = 1.0)$ and for $(Pr = 7.0)$. It is noticed from the graph that, the heat generating/absorbing parameter decrease the mass flow rate for all cases of K. **Figure 21** depict the effect of Grashof number on mass flow rate (Q) for cases $(K = 0.0, K = 0.5$ *and* $K = 1.0)$ and for $(Pr = 7.0)$. It is evident from the graph that, the thermal buoyancy force increase the mass flow rate for all cases of K.

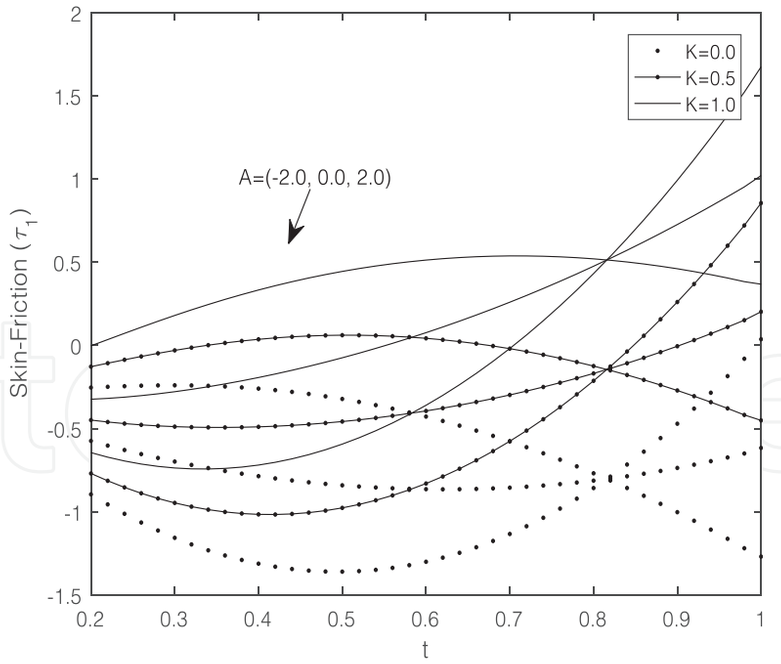

Figure 12.
Variation of skin friction (τ_1) *for different values of heat source/sink* $(A$ *and* $K)$ $(Pr = 7.0, \lambda = 2.0, M = 2.0$ $Gr = 5.0)$.

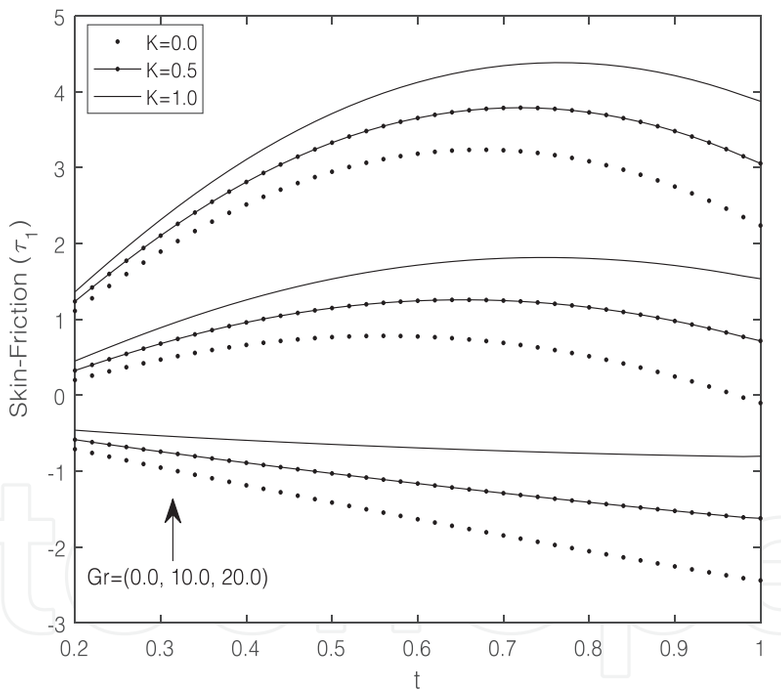

Figure 13.
Variation of skin friction (τ_1) *for different values of Grashof number* $(Gr$ *and* $K)$ $(Pr = 7.0, \lambda = 2.0, M = 2.0$ $Gr = 5.0, A = -2.0)$.

3. Conclusion

The study of MHD natural convection flow of constant heat source/sink in an annulus due to ramped motion and ramped temperature of the boundaries have been carried out. The Laplace transform techniques have been used and the time domain solution was obtained using the Riemann sum approximation. The effect of the governing parameters such as the Hartmann number (M), radii ratio (λ), time (t), Grashof number (Gr) Heat generating/absorbing parameter (A) and

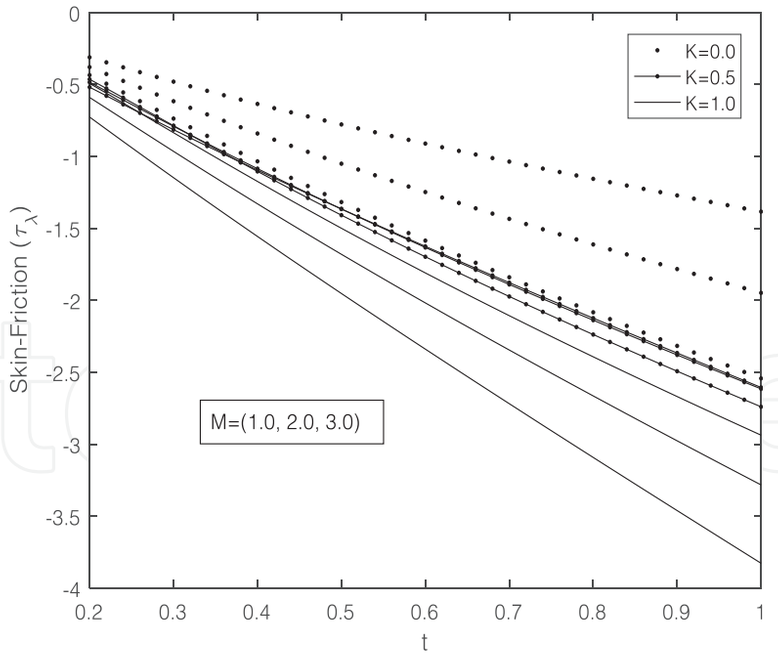

Figure 14.
Variation of skin friction (τ_λ) *for different values of Hartmann number* $(M$ *and* $K)(Pr = 7.0, \lambda = 2.0,$ $A = -2.0\ Gr = 5.0)$.

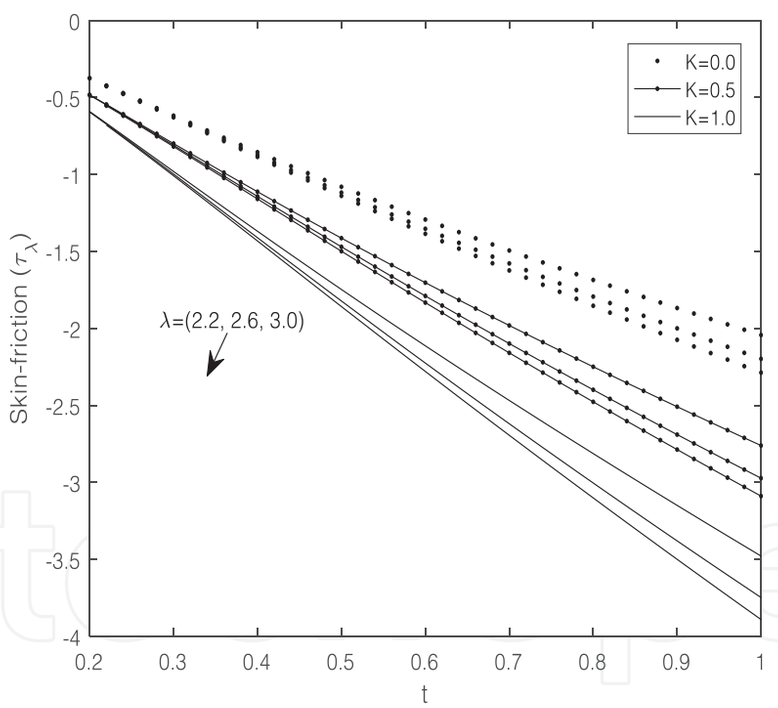

Figure 15.
Variation of skin friction (τ_λ) *for different values of radii ratio* $(\lambda$ *and* $K)$ $(Pr = 7.0, M = 2.0, A = -2.0$ $Gr = 5.0)$.

Prandtl number water $(Pr = 7.0)$ on the dimensionless fluid velocity (U), temperature (θ), mass flow rate (Q) and skin – friction $(\tau_1$ *and* $\tau_\lambda)$ at both surfaces of the cylinder considering three cases of the velocity of the magnetic field ($K = 0.0$ when the magnetic field is fixed relative to the fluid, $K = 0.5$ when the velocity of the magnetic field is less than the velocity of the moving cylinder and $K = 1.0$ when the magnetic field is fixed relative to the moving cylinder) have been analyzed with the help of line graphs.

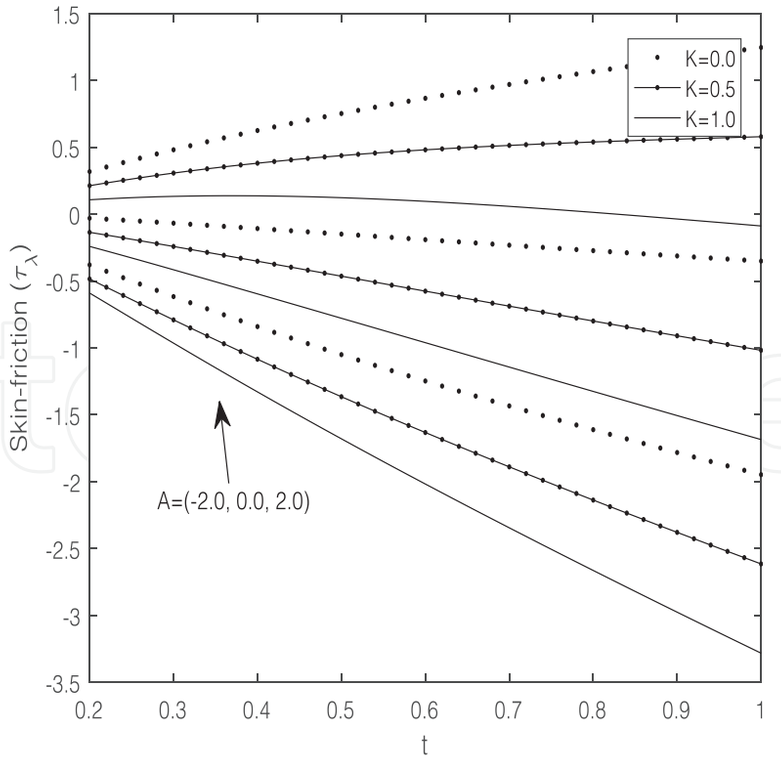

Figure 16.
Variation of skin friction (τ_λ) *for different values of heat source/sink* $(A \text{ and } K)(Pr = 7.0, M = 2.0, \lambda = 2.0$ $Gr = 5.0)$.

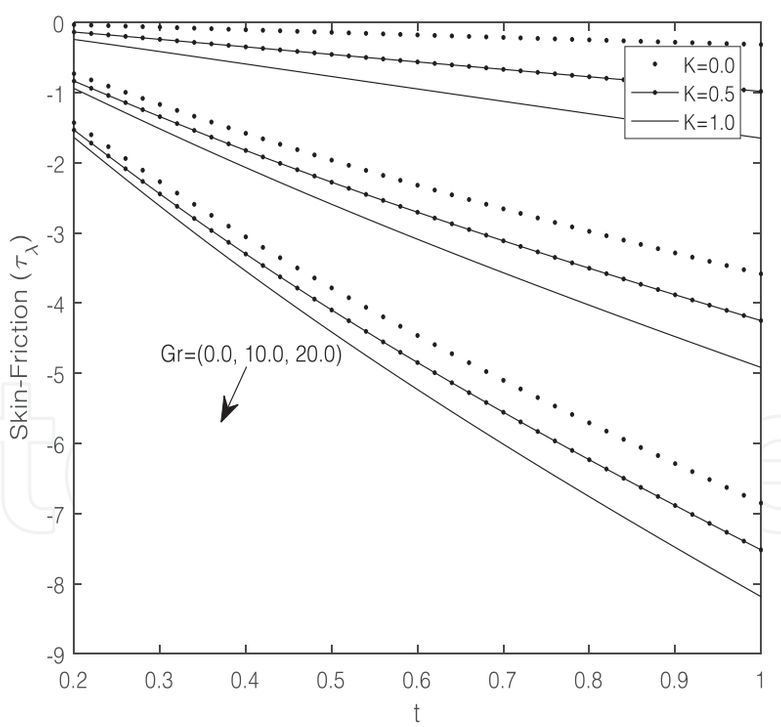

Figure 17.
Variation of skin friction (τ_λ) *for different values of Grashof number* $(Gr \text{ and } K)(K = 0.0, M = 2.0, \lambda = 2.0$ $A = -2.0)$.

The noteworthy conclusions are summarized as follows:

- Hartmann number has a retarding effect on the skin friction (τ_1) and mass flow rate. It also decreases fluid velocity for cases $(K = 0.0 \textit{ and } K = 0.5)$ the reverse

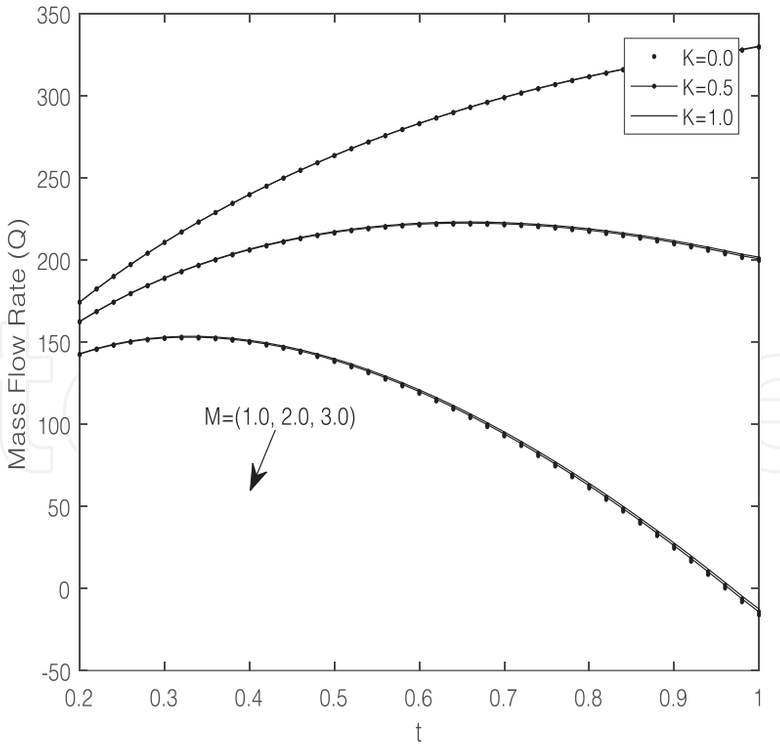

Figure 18.
Variation of mass flow rate (Q) *for different values of Hartmann number* $(M$ *and* $K)(K = 0.0, \lambda = 2.0,$ $A = -2.0, Gr = 5.0)$.

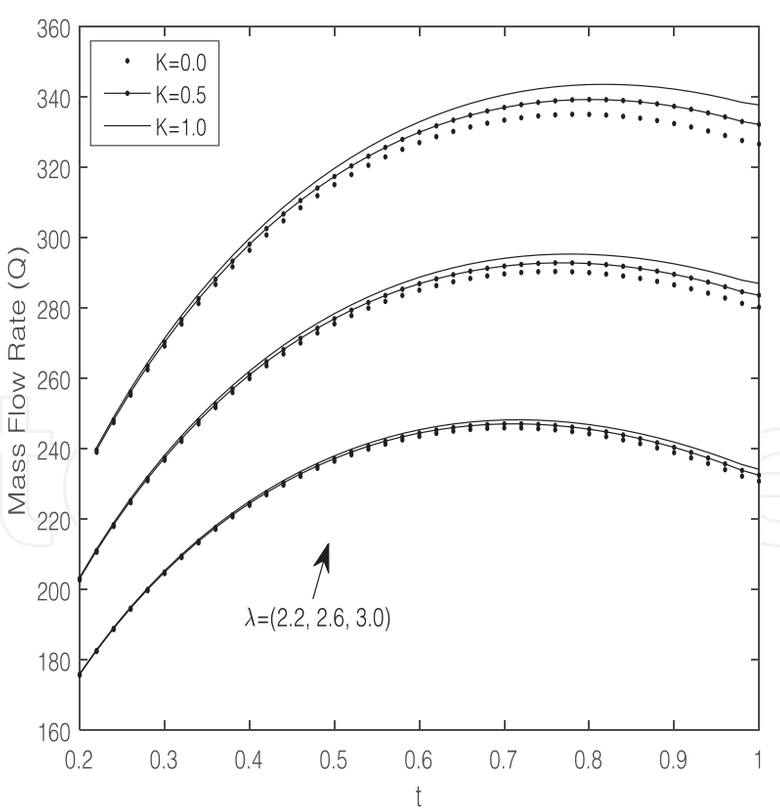

Figure 19.
Variation of mass flow rate (Q) *for different values of radii ratio* $(\lambda$ *and* $K)(K = 0.0, M = 2.0,$ $A = -2.0, Gr = 5.0)$.

effect is noticed for case $(K = 1.0)$. increase in Hartmann number lead to an increase in skin friction (τ_λ) for case $(K = 0.0)$ but decreases it for cases $(K = 0.0$ *and* $K = 0.5)$

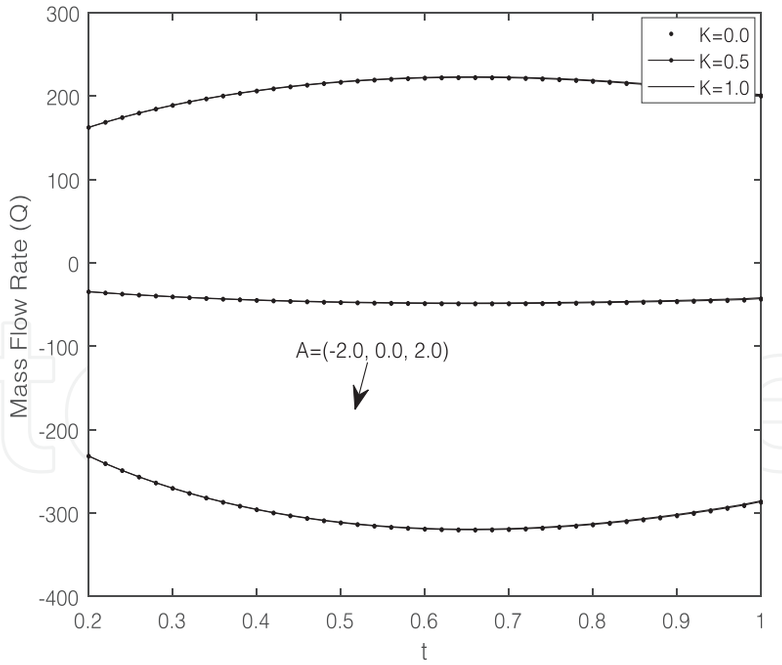

Figure 20.
Variation of mass flow rate (Q) *for different values of heat source/sink* $(A$ *and* $K)(K = 0.0, M = 2.0$ $\lambda = 2.0, Gr = 5.0)$.

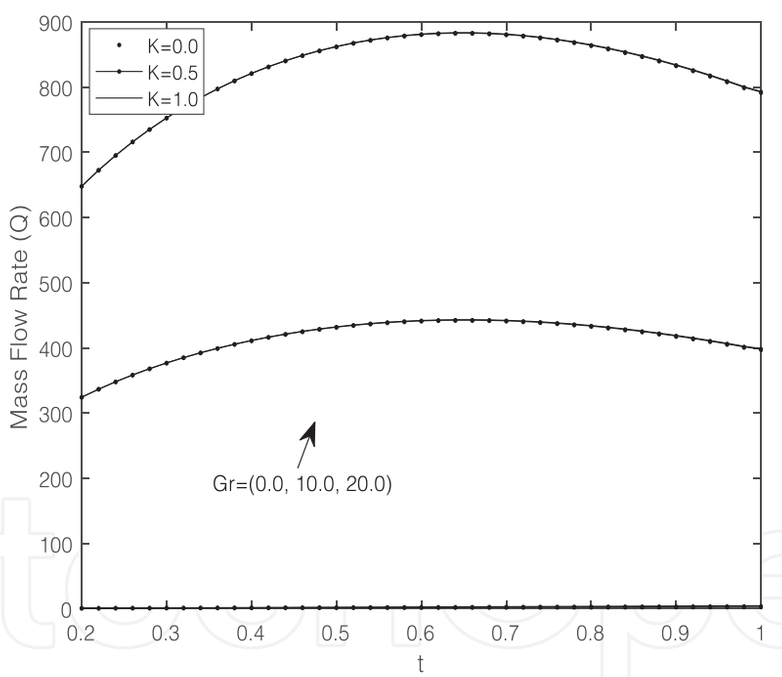

Figure 21.
Variation of mass flow rate (Q) *for different values of Grashof number* $(Gr$ *and* $K)(K = 0.0, M = 2.0,$ $\lambda = 2.0, A = -2.0)$.

- Thermal buoyancy force and radii ratio increase mass flow rate when $= 7.0$. As the radii ratio and Grashof number increase, there is an increase in fluid velocity and skin friction (τ_1) for all cases of K and for $Pr = 7.0$. The reverse effect occurs for skin friction (τ_λ). Radii ratio also increases the fluid temperature

- Heat generating/absorbing parameter has a retarding effect on fluid velocity, temperature and skin friction (τ_1) while it enhances the skin friction (τ_λ) for all cases of K and for $Pr = 7.0$. It decreases mass flow rate when $Pr = 7.0$.

Nomenclature

t'	Dimensional time (s)
u'	Velocity (m/s)
r'	Dimensional radial coordinate
U	Dimensionless velocity (m/s)
B_0	Constant magnetic flux density
T_0	Reference temperature (K)
I_n	Modified Bessel's function of first kind of order n
K_n	Modified Bessel's function of second kind of order n
T_w	Constant temperature (K)
M	Hartmann number
Pr	Prandtl number
Nu	Nusselt number
Gr	Grashof number
Q	Dimensionless volume flow rate $(kgs^{-1}m^{-2})$
a	Radius of the inner cylinder
b	Radius of the outer cylinder
t	Dimensionless time (s)
R	Dimensionless radial coordinate
g	Gravitational acceleration (m/s^2)
c_p	Specific heat at constant pressure $(J/kg/K)$

Greek letters

υ	Fluid kinematic viscosity (m^2/s)
τ	(Skin-friction)
ρ	Density (kg/m^3)
β	Coefficient of thermal expansion (K^{-1})
λ	Ratio of radii $(\frac{b}{a})$
σ	Electrical conductivity of the fluid $(W/m.K)$
α	Thermal diffusivity (m^2/s)
μ	Magnetic diffusivity (m^2/s)

Author details

Khadijah Lawal* and Haruna Jibril
Ahmadu Bello University Zaria, Kaduna State, Nigeria

*Address all correspondence to: khadijahlawal19@gmail.com

References

[1] Chandran P, Sacheti NC, Singh AK. Natural convection near a vertical plate with ramped wall temperature. Heat and Mass Transfer. 2005;**41**:459-464

[2] Jha BK, Samaila AK, Ajibade AO. Natural convection flow of heat generating/bbsorbing fluid near a vertical plate with ramped temperature. JEAS. 2012;**2**:61-68

[3] Seth GS, Ansari MS, Nandkeolyar R. MHD unsteady hydro-magnetic Couette flow within a porous channel. Tamkang Journal of Science and Engineering. 2011;**14**:7-14

[4] Nandkeolyar R, Das M. Unsteady MHD free convection flow of a heat absorbing dusty fluid past a flat plate with ramped wall temperature. Afrika Matematika. 2014;**25**:779-798

[5] Seth GS, Ansari MS, Nandkeolyar R. MHD natural convection flow with radiative heat transfer past an impulsively moving plate with ramped wall temperature. Heat and Mass Transfer. 2011;**47**:551-561

[6] Seth G, Hussain SM, Sarkar S. Hydro magnetic natural convection flow with heat and mass transfer of a chemically reacting and heat absorbing fluid past an accelerated moving plate with ramped temperature and ramped surface concentration through a porous medium. Bulgarian Chemical Communications. 2016;**48**:659-670

[7] Lawal KK, Jibril HM. Unsteady MHD natural convection flow of heat generating/absorbing fluid near a vertical plate with ramped temperature and motion. Journal of Taibah University for Science. 2019;**13**(1): 433-439

[8] Lawal KK, Jibril HM. Time dependent MHD natural convection flow of heat generating/absorbing fluid near a vertical porous plate with ramped boundary conditions. Euro Afro Studies International Journal. 2019;**1**(1):81-122

[9] Jha BK, Jibril HM. Hydro magnetic flow due to ramped motion of the boundary. International Journal of Applied Mechanics and Engineering. 2010;**15**:1101-1109

[10] Kumar A, Singh AK. Transient magneto hydrodynamic Couette flow with ramped velocity. International Journal of Fluid Mechanics. 2010;**I37**: 435-446

[11] Jha BK, Jibril H. Effect of transpiration on the MHD flow near a porous plate having ramped motion. Journal of the Physical Society of Japan. 2011;**80**:64684

[12] Jha BK, Jibril H. Time dependent MHD couette flow due to ramped motion of one of the boundaries. International Journal of Applied Mechanics. 2012;**17**(2):383-399

[13] Jha BK, Jibril H. Time dependent MHD Couette due to ramped motion of one the porous plate. International Journal of Applied Mechanics and Engineering. 2013;**18**(4):1039-1056

[14] Jha BK, Apere CA. Unsteady MHD Couette flow in annuli, the Riemann Sum approximation approach. Journal of Physical Society Japan. 2010;**79**: 124403 (5 pp.)

[15] Jha BK, Apere CA. Unsteady MHD two- phase Couette flow of fluid particles suspension in an annulus. AIP Advances. 2011;**1**:042121

[16] Anand. Effect of radial magnetic field on free convective flow over ramped velocity moving vertical cylinder with ramped type temperature and concentration. Fluid Mechanica. 2016;**9**(6):2655-2864

[17] Anand. Effect of radial magnetic field on natural convection flow in alternate conducting vertical concentric annuli with ramped temperature. Engineering Science and Technology. An International Journal. 2016;**19**(3): 1436-1451

[18] Anand. Effect of velocity of applied magnetic field on natural convection over ramped type moving inner cylinder with ramped type temperature. International Journal of Mechanica Sciences. 2017;**131**:625-632

[19] Taiwo YS. Exact solution of an MHD natural convection flow in vertical concentric annulus with heat absorption. International Journal of system engineering. 2017;**1**(1): 15-24

[20] Zakaria MN, Hussanan A, Khan I, et al. The effects of radiation on free convection flow with ramped wall temperature in Brinkman type fluid. Jurnal Teknologi. 2013;**62**:33-39

[21] Jha BK, Apere CA. Magneto hydrodynamic transient free convection flow in a vertical annulus with thermal boundary condition of second kind. International Journal of Heat and Mass Transfer. 2012;**134**(4):042502

[22] Tasawar H et al. Analytic solution for MHD flow in an annulus. Communications in Nonlinear Science and Numerical Simulation. 2010;**15**(5): 1224-1227

[23] Kundu PK, Das K, Acharya N. Flow features of a conducting fluid near an accelerated vertical plate in porous medium with ramped wall temperature. Journal of Mechanics. 2014;**30**:277-288

[24] Samiulhaq, Ahmed S, Vieru D, et al. Unsteady magnetohydrodynamic free convection flow of a second grade fluid in a porous medium with ramped wall temperature. PLoS. 2014;**9**:e88766

[25] Samiulhaq, Khan I, Ali F, et al. Free convection flow of a second-grade fluid with ramped wall temperature. Heat Transfer Research. 2014;**45**:579-588

[26] Seth GS, Nandkeolyar R, Ansari MS. Effect of rotation on unsteady on unsteady hydro magnetic natural convection flow past an impulsively moving vertical plate with thermal diffusion and heat absorption. International Journal of Applied Mathematics and Mechanics. 2011;**7**: 52-69

[27] Lawal KK, Jibril HM. Impact of relative motion of a magnetic field on unsteady magneto-hydrodynamic natural convection flow with a constant heat source/sink. Heat Transfer. 2020;**1**: 1-21. DOI: 10.1002/htj.21888

[28] Lawal KK, Jibril HM. Influence of relative motion of magnetic field on time-dependent MHD natural convection flow. Heat Transfer. 2020;**1**: 1-20. DOI: 10.1002/htj.21890

[29] Tzou DY. Macro to Micro Scale Heat Transfer: The Lagging Behavior. London: Taylor and Francis; 1997